

ORIGINAL ARTICLE

Lrs14 transcriptional regulators influence biofilm formation and cell motility of Crenarchaea

Alvaro Orell¹, Eveline Peeters², Victoria Vassen¹, Silke Jachlewski³, Sven Schalles¹, Bettina Siebers³ and Sonja-Verena Albers¹

¹Molecular Biology of Archaea, Max Planck Institute for terrestrial Microbiology, Marburg, Germany;

²Research Group of Microbiology, Department of Sciences and Bio-engineering Sciences, Vrije Universiteit Brussel, Pleinlaan 2, Brussels, Belgium and ³Molecular Enzyme Technology and Biochemistry (MEB), Faculty of Chemistry, Biofilm Centre, University of Duisburg-Essen, Universitätsstrasse 5, Essen, Germany

Like bacteria, archaea predominately exist as biofilms in nature. However, the environmental cues and the molecular mechanisms driving archaeal biofilm development are not characterized. Here we provide data suggesting that the transcriptional regulators belonging to the Lrs14-like protein family constitute a key regulatory factor during *Sulfolobus* biofilm development. Among the six *Lrs14*-like genes encoded by *Sulfolobus acidocaldarius*, the deletion of three led to markedly altered biofilm phenotypes. Although Δ *saci1223* and Δ *saci1242* deletion mutants were impaired in biofilm formation, the Δ *saci0446* deletion strain exhibited a highly increased extracellular polymeric substance (EPS) production, leading to a robust biofilm structure. Moreover, although the expression of the adhesive pili (*aap*) genes was upregulated, the genes of the motility structure, the archaellum (*fla*), were downregulated rendering the Δ *saci0446* strain non-motile. Gel shift assays confirmed that *Saci0446* bound to the promoter regions of *fla* and *aap* thus controlling the expression of both cell surface structures. In addition, genetic epistasis analysis using Δ *saci0446* as background strain identified a gene cluster involved in the EPS biosynthetic pathway of *S. acidocaldarius*. These results provide insights into both the molecular mechanisms that govern biofilm formation in Crenarchaea and the functionality of the Lrs14-like proteins, an archaea-specific class of transcriptional regulators.

The ISME Journal (2013) 7, 1886–1898; doi:10.1038/ismej.2013.68; published online 9 May 2013

Subject Category: Microbial population and community ecology

Keywords: archaea; biofilm formation; cell motility; EPS; transcriptional regulation

Introduction

The ability to form biofilms is considered the most prevalent means of microorganisms to persist in nature, enabling microbes to withstand a broad variety of environmental fluctuations such as temperature and pH changes, nutrient availability and the presence of toxins (Costerton *et al.*, 1995; Lopez *et al.*, 2010). Biofilms have been extensively studied in members of the bacteria as their presence can promote several persistent and chronic infections (Costerton *et al.*, 1999). In contrast, it is rather recent that environmental biofilms built up of archaeal and bacterial species are being examined, mainly due to their relevance in biogeochemical cycling of essential elements (Shock *et al.*, 2005; Justice *et al.*, 2012).

Archaea form biofilms within many microbial ecosystems such as acid mine drainage sites, seafloor sediments or acidic hot springs mats (Baker and Banfield, 2003; Orcutt *et al.*, 2011); Kozubal *et al.*, 2012). Initial description of the archaeal biofilms were reported in the euryarchaeota *Archaeoglobus fulgidus* (Lapaglia and Hartzell, 1997) and in the bi-species biofilm of *Pyrococcus furiosus* and *Methanopyrus kandlerii* (Schopf *et al.*, 2008). *Ferroplasma acidarmanus* displayed a multi-layered biofilm and proteomic studies revealed upregulation of proteins involved in the adaptation to anoxia indicating existence of anaerobic zones in the multilayered biofilms (Baker-Austin *et al.*, 2010). Morphologies of different haloarchaeal biofilms ranged from carpet-like to multi-layered biofilms containing micro- and macro-colonies as well as biofilms characterized by large aggregates of cells able to attach to abiotic surfaces (Fröls *et al.*, 2012).

Three crenarchaea *S. acidocaldarius*, *S. solfataricus* and *S. tokodaii* displayed very diverse biofilm morphologies: either simple carpet-like structures in *S. solfataricus* or highly dense tower-like structures in *S. acidocaldarius* communities (Koerdt *et al.*,

Correspondence: SV Albers, Molecular Biology of Archaea, Max Planck Institute for terrestrial Microbiology, Karl-von-Frisch-Strasse, Marburg, D-35043, Germany.

E-mail: albers@mpi-marburg.mpg.de

Received 27 December 2012; revised 13 March 2013; accepted 15 March 2013; published online 9 May 2013

2010). Proteomic studies conducted on biofilms grown as static biofilms of *S. acidocaldarius*, *S. solfataricus* and *S. tokodaii* showed that only seven changes were shared across the three strains (Koerdt *et al.*, 2011). One of the most striking common response genes included the putative Lrs14-like transcriptional regulators indicating their possible role as regulatory factors during biofilm development of *Sulfolobus* spp.

Although an Lrs14 protein-encoding gene was previously identified and isolated from *S. solfataricus* (Napoli *et al.*, 1999), its physiological target genes are unknown. *S. solfataricus* Lrs14 was found to be negatively auto-regulated and accumulated in late growth phases (Napoli *et al.*, 1999). In contrast to other known metal-dependent regulators inhibition occurred in a ligand-independent manner (Bell and Jackson 2001).

In this study, we investigated the effect of the deletion of six Lrs14 transcriptional regulators during biofilm development of *S. acidocaldarius*. Mutational analysis combined with both phenotypic and *in vitro* characterization of the six homologous Lrs14 proteins encoded by *S. acidocaldarius* revealed that three of them significantly influenced either biofilm formation or cell motility. For one homolog, *saci0446*, it was shown that its absence strongly impaired cell motility and promoted extracellular polymeric substance (EPS) overproduction, thus leading to an enhanced biofilm formation. This report provides for the first time insights into transcriptional regulation of archaeal biofilm development.

Materials and methods

S. acidocaldarius strains and growth conditions

S. acidocaldarius MW001 (Wagner *et al.*, 2012) and all in-frame marker-less deletion mutants were aerobically grown at 76 °C in Brock media (Brock *et al.*, 1972), pH 3 and supplemented with 0.1% (w/v) N-Z-amine and 10 mg ml⁻¹ uracil. Uracil was not added to the media for cultivation of *S. acidocaldarius* MW001^{pyrEF+} and *pyrEF* disruption mutants. For protein overproduction experiments in *S. acidocaldarius*, 0.4% (w/v) maltose was added to the media to induce expression. Growth progression was monitored by the measurement of the optical density at 600 nm (OD₆₀₀). All *S. acidocaldarius* deletion strains are described in Table 1.

Methods for protein alignments, the construction of plasmids for deletion mutants and the genetic manipulation of *S. acidocaldarius* are described in the Supplementary Material. Oligonucleotides employed for these procedures are listed in Supplementary Table 1.

Microtitre plate assays

A microtitre plate assay using polystyrol 96-well tissue culture plates (flat bottom cell+, Sarstedt,

Nuembrecht, Germany) adapted to high temperature as developed by Koerdt *et al.*, 2010 was performed. After 2 days incubation, microtitre plates were cooled down to room temperature and the efficiency of biofilm formation was calculated by the correlation of the measured crystal violet absorbance of attached cells (OD₅₇₀) and growth of planktonic cells (OD₆₀₀). At least eight plates were used for both deletion and reference strains. The results were represented as percentage of biofilm formation of the *S. acidocaldarius* Lrs14 deletion mutant strains relative to either *S. acidocaldarius* MW001 or MW001^{pyrEF+} reference strains.

Biofilm culturing and confocal laser scanning microscopy (CLSM) analysis

Static biofilm cultures of *S. acidocaldarius* strains were grown in small Petri dishes (μ-dishes, 35 mm, Ibbidi, Martinsried, Germany) in Brock media supplemented with 0.1% (w/v) N-Z amine and 10 mg ml⁻¹ of uracil when necessary. For over-expressing strains 0.2% (w/v) maltose was added. All strains were inoculated at 0.01 OD₆₀₀ and two biological replicates of each strain were grown for 3 days at 75 °C. The medium was carefully exchanged every 24 h to ensure aerobic growth conditions and nutrient replenishment. Petri dishes were put in a specially designed metal box (25 cm L × 20 cm W × 20 cm D) filled with ~500 ml of water in the bottom to minimize evaporation of the media, as described by Koerdt *et al.* (2010). Biofilms were imaged as described in Koerdt *et al.* (2012).

To evaluate cell surface coverage of the biofilms, pictures of the bottom layer were taken using a differential interference contrast objective. Twelve images at different microscopy fields were recorded. By using Adobe Photoshop CS2 software differential interference contrast pictures were converted into black/white in order to calculate number of pixels/area, thus representing the percentage surface coverage. Cell surface coverage determinations were performed in three biological replicates.

Swimming motility on semi-solid gelrite plates

Swimming motility on plates was analyzed on semi-solid gelrite plates consisting of 0.15% gelrite supplemented with 0.001% (w/v) NZ-amine and 0.4% (w/v) maltose when necessary. Cells grown in standard Brock medium were harvested during exponential growth and used to inoculate plates at a cell density of 10⁷ cells per ml. Plates were incubated for 7 days in a humid chamber at 75 °C. Swimming behavior of the different *S. acidocaldarius* strains was analyzed by measuring the swimming radius.

RNA isolation and quantitative reverse transcription-PCR (qRT-PCR)

Total RNA samples were isolated from 10 ml of exponentially growing shaking culture (OD₆₀₀ = 0.2),

Table 1 Strains and plasmids

Strain/plasmid	Genotype	Source/reference
<i>Strain</i>		
<i>E. coli</i>		
DH5 α	<i>Escherichia coli</i> K-12 cloning strain	Gibco (Carlsbad, CA, USA)
ER1821	F- <i>glnV44 e14-(McrA-)</i> <i>rfdD1 relA1 endA1 spoT1</i>	New England Biolabs (Ipswich, MA, USA)
BL21(DE3)	<i>thi-1 Δ(mcrC-mrr)114::IS10E. coli B F-ompT hsdS(r_B-m_B-) dcm +</i>	Agilent Technologies (Boeblingen, Germany)
RIL	Tet ^r gal λ <i>endA Hte [argU ileY leuW Cam^r]</i>	
<i>S. acidocaldarius</i>		
DSM639	<i>S. acidocaldarius</i>	DSMZ
MW001	Deletion of <i>pyrEF</i> (91-412 bp) in <i>S. acidocaldarius</i>	Wagner <i>et al.</i> (2012)
MW001 ^{pyrEF+}	MW001 chromosomally complemented with <i>pyrEF</i>	Wagner and Albers, unpublished
MW250	Deletion of <i>saci0102</i> in MW001	This study
MW251	Deletion of <i>saci0446</i> in MW001	This study
MW253	Deletion of <i>saci1242</i> in MW001	This study
MW254	Deletion of <i>saci1223::pyrEF</i> in MW001	This study
MW255	Deletion of <i>saci1219::pyrEF</i> in MW001	This study
MW256	Deletion of <i>saci0133::pyrEF</i> in MW001	This study
MW261	Deletion of <i>saci0446</i> and <i>saci1908</i> in MW001	This study
MW262	Deletion of <i>saci0446</i> and <i>saci1908</i> in MW001	This study
MW263	MW251 (<i>Δsaci0446</i>) carrying pSVA2024	This study
MW264	MW251 (<i>Δsaci0446</i>) carrying pSVA2026	This study
MW019	Deletion of <i>saci1172 (fla)</i> in MW001	Lassak <i>et al.</i> (2012)
<i>Plasmid</i>		
pSVA406	Gene targeting plasmid, pGEM-T Easy backbone, <i>pyrEF</i> cassette of <i>S. solfataricus</i>	Wagner <i>et al.</i> (2012)
pSVA452	In-frame deletion of <i>saci0446</i> cloned into pSVA406 with <i>Apal</i> , <i>PstI</i>	This study
pSVA453	In-frame deletion of <i>saci0102</i> cloned into pSVA406 with <i>Apal</i> , <i>BamHI</i>	This study
pSVA2004	In-frame deletion of <i>saci1242</i> cloned into pSVA406 with <i>Apal</i> , <i>BamHI</i>	This study
pMZ1	C-terminal strep-10x histag, pSVA5 derivative	Zolghadr <i>et al.</i> (2007)
pSVA1450	pRN1-based shuttle vector with <i>lacS</i> reporter gene of <i>S. solfataricus</i>	Wagner and Albers, unpublished
pSVA2022	<i>saci0446</i> ORF cloned into pMZ1 with <i>NcoI</i> , <i>BamHI</i>	This study
pSVA2024	<i>saci0446</i> ORF and own promoter sequence cloned into pSVA1450 with <i>SacII</i> , <i>EagI</i>	This study
pSVA2026	<i>saci0446</i> ORF cloned into pSVA1450 with <i>NcoI</i> , <i>EagI</i>	This study
pETDuet-1	<i>Amp^r</i> , <i>Car^r</i> , expression plasmid containing replicon ColE1 (pBR322) and two MCS (MCS1 and MCS2)	Novagen
pSVA2009	<i>saci0446</i> ORF cloned into pETDuet-1 with <i>NotI</i> , <i>EcoRI</i>	This study

10 ml of shaking culture at stationary phase (OD₆₀₀ = 0.4) and 40 ml of 3 days mature biofilm culture. To preserve RNA integrity, biofilm-containing Petri dishes were cooled down on ice before isolation and shaking cultures were immediately harvested by centrifugation at 4 °C. TRIzol reagent (Invitrogen, Carlsbad, CA, USA) was used for total RNA isolation following manufacturer's instructions. The preparation of the complementary DNA and the qRT-PCR were performed as described in Lassak *et al.*, 2012. Cq values of each transcript of interest were standardized to the Cq value of the housekeeping gene *saci0574 (secY)*; Van Der Sluis *et al.*, 2006). Quantitative PCR reactions with DNA-free RNA as template were performed as control. Primers used for quantitative PCR reactions are listed in Supplementary Table 1. At least three biological replicates of each assessed condition and two technical replicates per quantitative PCR reaction were performed.

EPS isolation and quantization

For EPS extraction, *S. acidocaldarius* strains MW001, MW251 and MW264 were grown as static biofilm cultures in 70 ml Brock media using 150 mm

diameter polystyrene Petri dishes (Sarstedt). Brock medium was supplemented with 0.4% maltose when necessary to induce protein expression. After 3 days of incubation at 76 °C, biofilms of each strain were scraped off from four Petri dishes and washed three times with 10 ml phosphate buffer (6 mM, pH 7). EPS were then isolated using the cation exchange resin Dowex (Sigma-Aldrich, Munich, Germany) as described previously for the isolation of EPS from *S. solfataricus* biofilms (Koerdt *et al.*, 2012). Carbohydrates ≥ 3.5 kDa were considered as high molecular weight.

Expression, purification and activity tests with *saci0446* are described in the Supplementary Material. Oligonucleotides employed for the construction of expression plasmids are listed in Supplementary Table 1.

Results

Lrs14-like proteins are an archaea-specific class of transcriptional regulators

BLAST searches using *Saci1223*, a putative *Lrs14*-like protein from *S. acidocaldarius*, as query revealed that hits showing $\geq 80\%$ of query sequence

coverage only matched to archaeal amino-acid sequences, corresponding to 58 crenarchaeal sequences (expected value $\leq 3e-04$) and 19 euryarchaeal homologous sequences (expected value $\leq 8e-04$). Only one bacterial sequence was retrieved when using Saci1223, which was a putative transcriptional regulator (YP_004180336.1; expected value of $7e-04$), encoded by the moderate thermophilic bacterium *Isosphaera pallida*, which shared 30% of identity with Saci1223. In addition, the BLASTP analysis determined that *S. acidocaldarius* genome encodes for six homologous Lrs14-like proteins: Saci1223, Saci0102, Saci0133, Saci0446, Saci1219 and Saci1242. These homologous proteins share identities from 34% to 39%.

Lrs14 proteins were formerly described as a bacterium-type transcriptional regulator related to the Lrp/AsnC (leucine-responsive regulatory protein) family of transcriptional regulators (Napoli *et al.*, 1999). Sequence alignment analysis together with secondary structure predictions revealed that the Lrs14 proteins lacked the C-terminal RAM domain (a $\beta\alpha\beta\beta\alpha\beta$ -fold motif), which is the distinctive ligand-binding domain of Lrp/AsnC-like proteins (Peeters and Charlier, 2010; Supplementary Figure 1A). Moreover, a neighbor joining distance analysis of archaeal Lrs14 and Lrp/AsnC regulators demonstrated that each subset of transcriptional regulators clustered in two well-defined clades, further supporting the distinctiveness between Lrs14-like and Lrp/AsnC as two divergent classes of regulators (Supplementary Figure 1B). Taking our analysis into account, we propose to categorize Lrs14-like proteins as a distinct type of archaea-specific class of transcriptional regulators.

Biofilm-associated transcriptional profile of *S. acidocaldarius* *lrs14* genes

Previously, two of the six *lrs14* genes (*saci1223* and *saci1242*) present in the *S. acidocaldarius* genome were found to be upregulated in biofilm-associated cell populations when compared with their planktonic counterparts (Koerdts *et al.*, 2011). To obtain the expression profiles of all six *S. acidocaldarius* *lrs14* genes, RNA was isolated from cells grown as 3-day-old biofilms or as planktonic shaking culture either in the exponential and late stationary phase. The expression of each *lrs14* gene was then determined as relative to the transcript levels found at the exponential growth phase. As shown in Figure 1, transcript levels of all six Lrs14-encoding open reading frames were increased both in the stationary growth phase and during biofilm growth. The expression of all six *lrs14* genes was enhanced at least twofold in the stationary phase (Figure 1). The *S. solfataricus* Lrs14 (SSO1101) also showed higher transcript levels at late growth stages (Napoli *et al.*, 1999). The most noteworthy changes were observed for *saci0446*, *saci1223* and *saci1242*, which were highly induced in *S. acidocaldarius* biofilms (9, 7

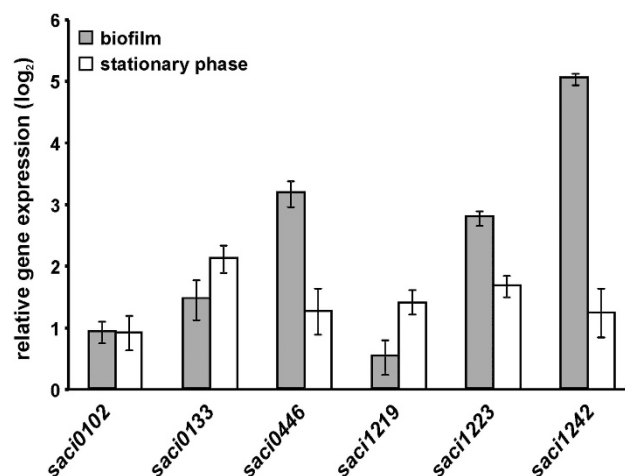


Figure 1 Expression profile of *S. acidocaldarius* *lrs14* genes during both biofilm and planktonic growth. Total RNA isolated from *S. acidocaldarius* MW001 and MW001^{pyrEF+} (reference strains) grown either as biofilms or as planktonic cultures were used for complementary DNA (cDNA) synthesis. qRT-PCR analysis was performed using specific primers for each Lrs14-encoding ORF (shown underneath the plot). Relative transcript expression levels of each gene were normalized to the internal control gene *secY*. The values reflect the fold change in gene expression compared with cDNA prepared from exponential grown planktonic reference strains cells, which is designated as baseline. The means and standard deviations of three biological replicates are shown.

and 32-fold changes, respectively). The same gene expression profile was observed when comparing the biofilm-associated cell population versus its planktonic cell population counterpart (Supplementary Figure 2). These gene expression patterns implied a potential role of Lrs14 proteins Saci0446, Saci1223 and Saci1242 during biofilm development.

Biofilm formation of *S. acidocaldarius* *lrs14* single deletion mutants

To understand the *in vivo* function of the Lrs14 proteins, single deletion mutants of all six *lrs14* putative genes were constructed in *S. acidocaldarius*. Using the marker-less mutant method in the uracil auxotrophic *S. acidocaldarius* mutant MW001 as reference strain (Wagner *et al.*, 2012), in-frame deletion mutants were obtained for *saci0102*, *saci0446* and *saci1242*. As this strategy was not successful for the construction of *saci0133*, *saci1223* and *saci1219*, these ORFs were deleted by a single homologous recombination step disrupting each gene via the insertion of the *pyrEF* selection cassette. The identity of each mutant strain was confirmed by PCR amplification of the appropriate genomic region and the subsequent sequencing (Supplementary Figure 3).

Analysis of the growth curves in shaking cultures revealed no obvious difference in the growth kinetic of the deletion mutants compared with the respective reference strains, MW001 (for in-frame deletion mutants) or MW001^{pyrEF+} (for *pyrEF* disruption mutants; Supplementary Figure 4). Only slightly lower cell densities at the stationary phase were

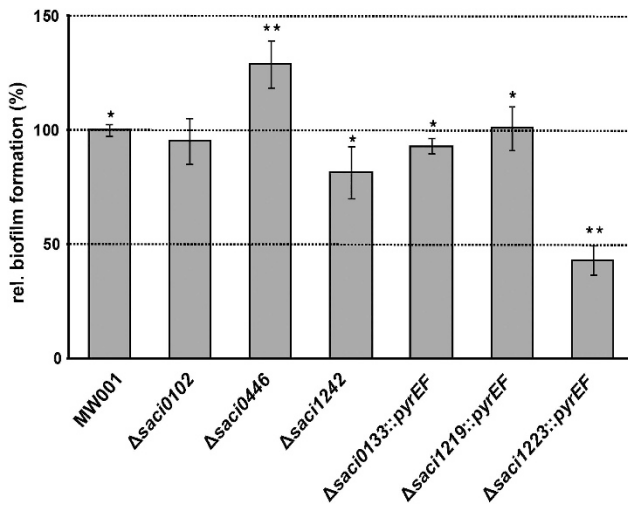


Figure 2 Biofilm formation of the *S. acidocaldarius* *Lrs14* deletion mutants by microtitre plate assays. Biofilm formation of each strain was calculated by the correlation of the measured crystal violet absorbance of attached cells (OD_{570}) and growth of planktonic cells (OD_{600}) to emphasize the amount of cells in a sessile lifestyle. The graph shows biofilm formation as relative to the wild-type strain MW001, which represented 100%. Each point and standard deviation is the mean of at least eight plates per condition. *Significant $P \leq 0.05$, **highly significant $P \leq 0.01$.

observed for Δ saci0446, Δ saci1242, Δ saci0133 and Δ saci1219 deletion strains (Supplementary Figure 4). Interestingly, the diminished biomass shown by the Δ saci0133 and Δ saci1219 deletion strains at late growth stages correlated with the higher transcript levels found in the stationary growth (Figure 1). In addition, no morphological defects could be observed when *Lrs14* deletion mutant strains cells were subjected to optical microscopic analysis (data not shown).

The ability of *Lrs14* deletion strains to form static biofilms was assessed by means of a microtiter plate assay adapted to high temperatures (Koerdts *et al.*, 2010). After 3 days of static biofilm formation, three out of the six deletion mutants showed significant alterations (Figure 2). Although Δ saci1223 showed a 60% decrease in biofilm formation, in the Δ saci0446 mutant 40% more biofilm was formed compared with the reference strain. In addition, biofilm formation by the Δ saci1242 mutant was reduced by 20% when compared with the reference strain (Figure 2). Mutant strains Δ saci0102, Δ saci0133 and Δ saci1219 revealed no significant differences in biofilm formation (Figure 2). Taken together, these results strongly suggested that *Lrs14* transcriptional regulators *Saci1223*, *Saci0446* and *Saci1242* have a role during development of *S. acidocaldarius* biofilm communities.

Comparative analysis of biofilm architectures formed by *S. acidocaldarius* *Lrs14* deletion mutants

In order to examine the morphologies of the biofilms formed by the *Lrs14* deletion mutants, the reference strains (MW001 and MW001^{pyrEF+}) and the *Lrs14*

deletion mutants were grown as static biofilms for 3 days. Although 4'-6-diamidino-2-phenylindole was used for visualization of cells within the biofilms, the presence of extracellular polysaccharide residues was detected using fluorescently labeled lectins that specifically bound to mannose/glucose (ConA) and galactosyl sugar residues (IB4). In Figure 3a, 4'-6-diamidino-2-phenylindole signal images (left column) or the overlay images of the three fluorescent signals are depicted (right column). Moreover, the surface coverage of each biofilm formed by the investigated strains was determined (Figure 3b).

As described by Henche *et al.* (2011), after 3 days of growth reference strain MW001 showed a confluent dense biofilm, displaying an EPS pattern in which the ConA (mannose/glucose) signal was dominant (Figure 3). Biofilm communities formed by MW001^{pyrEF+} showed no differences in comparison with MW001 (Supplementary Figure 5). Deletion mutants Δ saci0102 and Δ saci0133 showed biofilm architectures resembling the reference strain biofilm phenotype. Only slight differences were distinguishable as moderate lower cell density or less EPS production, leading to a decrease in biofilm heights when compared with the wild type (Figure 3). Δ saci1219 displayed a rather uneven biofilm phenotype in comparison with the reference strain (Figure 3). As expected from the microtitre plate assays, strains Δ saci1223, Δ saci0446 and Δ saci1242 showed pronounced morphological differences when forming biofilms. A poorly cell-colonized surface was observed for the biofilms of Δ saci1223 and Δ saci1242 deletion strains as observed by 4'-6-diamidino-2-phenylindole signal and the percentage of surface coverage of each strain (Figure 3). In addition, although Δ saci1223 produced only small amounts of EPS, Δ saci1242 displayed a particular cloud-like EPS pattern unevenly distributed on top of the biofilm (Figure 3). In contrast, the deletion of *saci0446* resulted in a densely packed biofilm structure. Although Δ saci0446 biofilm phenotype resembled the one displayed by the reference strain in terms of cell density, biofilm height and cell surface coverage, EPS production was notably increased by this mutant (see below), as clouds of mannose/glucose-rich EPS regularly distributed on top of the biofilm was visualized (Figure 3a).

The deletion of *saci1223*, *saci1242* and *saci0446* had a clear impact on formation and structures of *S. acidocaldarius* biofilm communities. In the deletion strains Δ saci1223, Δ saci1242 biofilm formation was impaired whereas the Δ saci0446 deletion strain exhibited a highly increased production of EPS leading to an enhanced biofilm formation.

Lrs14 protein *Saci0446* controls cell motility of *S. acidocaldarius*

S. acidocaldarius exhibits three distinct type IV pili-like structures on its surface: (i) the archaeellum,

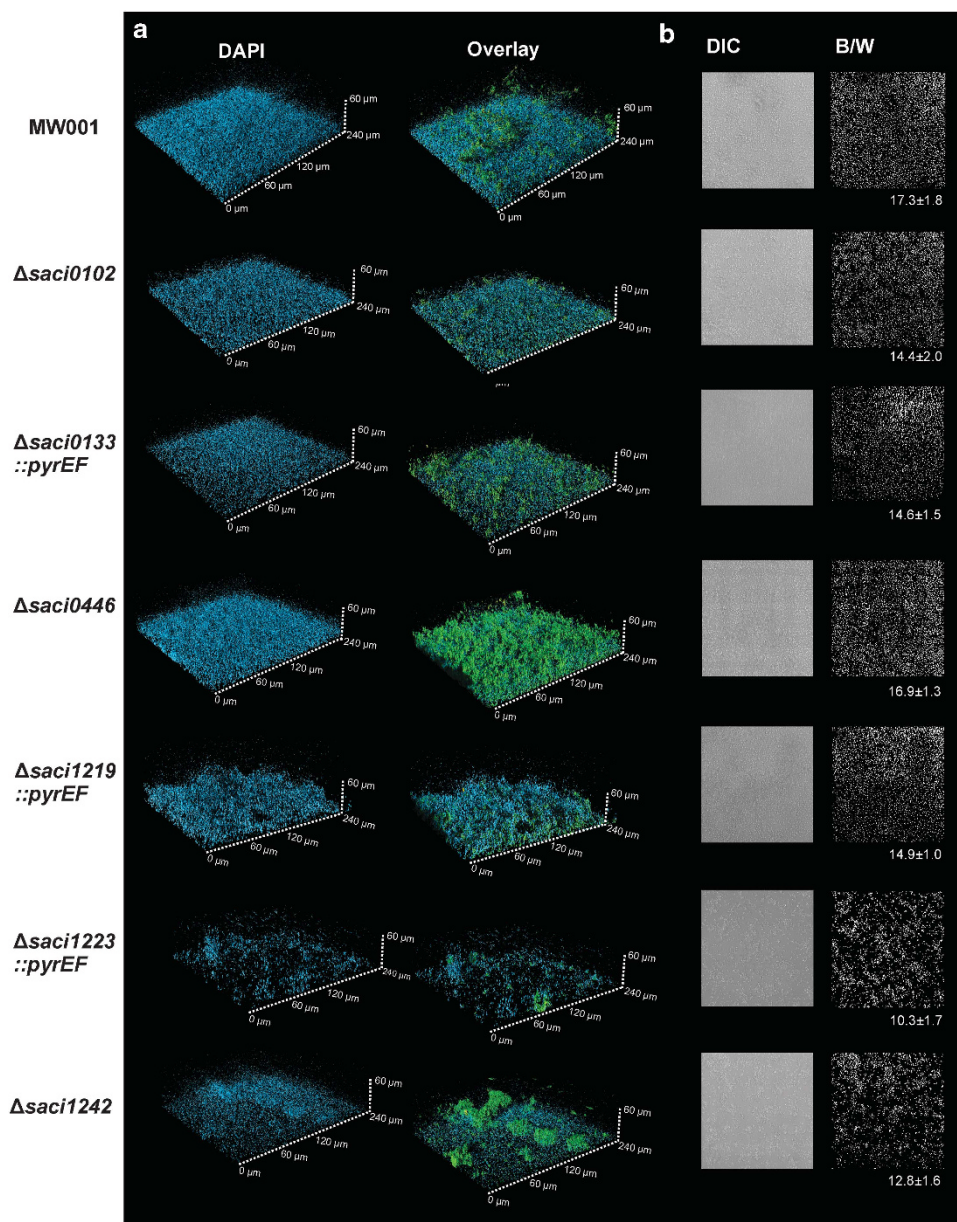


Figure 3 CLSM analysis of biofilm formed by the *S. acidocaldarius lrs14* deletion mutants. **(a)** Three-day-old biofilms were subjected to CLSM. The blue channel is the 4'-6-diamidino-2-phenylindole (DAPI) staining. The green channel represents the fluorescently labeled lectin ConA that binds to glucose and mannose residues. The lectin IB4 able to bind to α -galactosyl residues is shown in yellow. Overlay images of all three channels are shown. **(b)** Differential interference contrast (DIC) pictures (left panel) were taken from the bottom layer of biofilms and converted into black/white (B/W; right panel) to calculate the surface coverage. Numbers represent the percentage of surface coverage for each mutant strain.

(ii) the ultraviolet-induced pili and (iii) the adhesive pili aap. All three cell surface appendages played a role in surfaces colonization and the interplay of the three structures is important for the MW001 biofilm phenotype (Henche *et al.*, 2011). Therefore, it was important to determine whether the deletion of *saci1223*, *saci1242* or *saci0446* led to an altered synthesis of any of these cell surface appendages and therefore to the observed *Lrs14* deletion mutant biofilm phenotypes.

Using qRT-PCR, the expression levels of gene-encoding components, which are essential for the

assembly of each cell surface appendage (Henche *et al.*, 2011), were determined in 3-day-old biofilm communities of Δ *saci1223*, Δ *saci1242* and Δ *saci0446*, respectively. We determined that none of the tested cell surface appendage genes were differentially expressed in the Δ *saci1242* deletion strain as their transcript levels were found to not be significantly altered (considering a threshold of $\geq \pm 2$ -fold changes; Figure 4a). A similar expression pattern was observed for the Δ *saci1223* mutant, where only the expression of *upsA* and *upsE* (ultraviolet-induced structural component-encoding

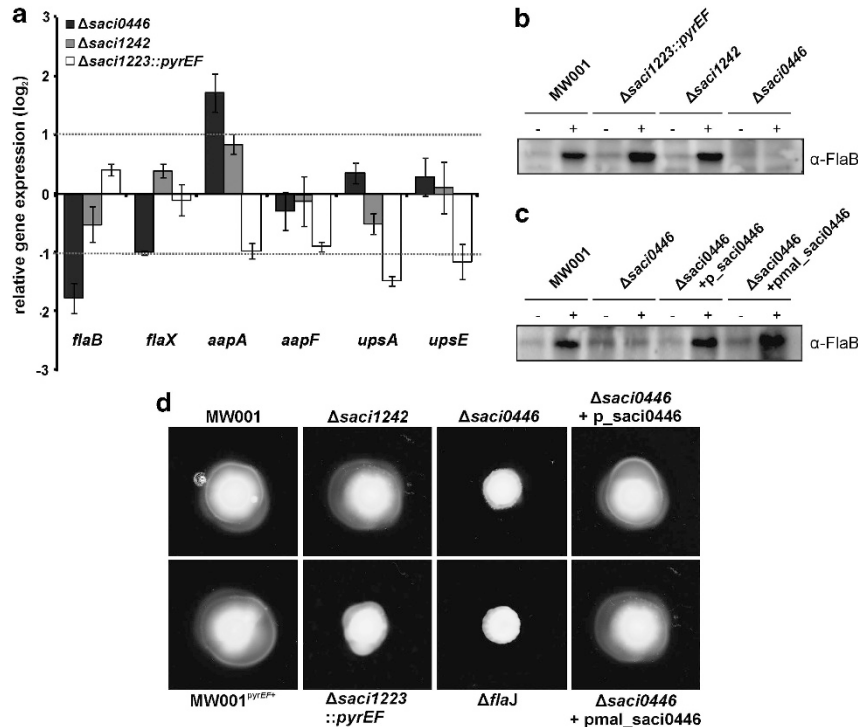


Figure 4 Effect of *S. acidocaldarius* *Lrs14* deletion mutants on cell motility. (a) qRT-PCR experiments to determine gene expression of components of the archaellum (*flaB* and *flaX*), aap pili (*aapA* and *aapF*) and ultraviolet-induced pili (*upsA* and *upsE*) in the deletion strains Δ *saci0446* (black bars), Δ *saci1242* (gray bars) and Δ *saci1223* (white bars) during biofilm growth. Relative transcript expression levels of each target gene were normalized to the internal control gene *secY*. The values reflect the fold change in expression compared with the reference strain MW001, which is designated as baseline. The means and s.d. of three biological replicates are shown. (b, c) FlaB expression levels were detected in *Lrs14* deletion mutants by immunoblotting with specific antibodies before (–) and after (+) induction via tryptone starvation. (d) Motility assay of *Lrs14* deletion mutants in comparison to the reference strain MW001 and MW001^{pyrEF+}. The non-motile strain Δ *flaJ* was included as a negative control. Trans-complemented strains of Δ *saci0446* are shown.

genes) were determined as downregulated (2.8- and 2.2-fold changes, respectively; Figure 4a).

In contrast, transcript levels of *flaB* and *flaX* (essential components of the archaellum) were downregulated in Δ *saci0446* biofilms (3.4- and 2.0-fold changes, respectively; Figure 4a), whereas transcript levels of *aapA* (3.4-fold changes), one of the two pilins forming the adhesive pilus, were increased (Figure 4a). Interestingly, this transcription profile resembled the one described for the *S. acidocaldarius* Δ *flaJ* strain (a non-archaellated strain) as it showed an increase of *aapA* and *aapB* transcript levels when grown as biofilms (Henche *et al.*, 2011). The overexpression of *aapA* in the Δ *saci0446* deletion strain might contribute its ability to form a more dense and stable biofilm because of the role of this adhesive appendage in both surface attachment and the establishment of cell-to-cell connections (Henche *et al.*, 2011).

To test the presumably regulatory role of *Saci0446* in archaellum expression, protein levels of FlaB, the structural protein of the archaellum, were determined in Δ *saci0446*, Δ *saci1223* and Δ *saci1242* in tryptone-starved cells, as it has been shown previously that upon starvation biosynthesis of all archaellum subunits is initiated (Lassak *et al.*, 2012). Expression levels of FlaB were the same in

Δ *saci1223* and Δ *saci1242* deletion strains compared with the reference strain (Figure 4b), whereas the accumulation of FlaB was hardly visible in the Δ *saci0446* deletion strain (Figure 4b). Moreover, FlaB wild-type proteins levels could be restored in trans-complemented Δ *saci0446* deletion strains by using a plasmid harboring the *saci0446* coding sequence including either its own promoter (Δ *saci0446* + p_{*saci0446*}) or a maltose inducible promoter (Δ *saci0446* + p_{mal}*saci0446*; Figure 4c).

To confirm that the deletion mutant Δ *saci0446* lacks archaella, its ability to swim on semi-solid gelrite plates containing reduced amounts of tryptone (0.005%) was tested. Motility of the Δ *saci0446* deletion strain was decreased to levels, which were comparable with the non-motile *S. acidocaldarius* mutant strain Δ *flaJ* (Lassak *et al.*, 2012; Figure 4d). Motility of Δ *saci0446* cells could be trans-complemented with the gene under control of its own or the *malE* promoter (Figure 4d). In addition, the Δ *saci1242* deletion strain showed a swimming radius comparable to the reference MW001, whereas Δ *saci1223* motility was slightly impaired (Figure 4c). In conclusion, *Saci0446* is involved in regulating motility of *S. acidocaldarius*, most likely by controlling expression of archaella components.

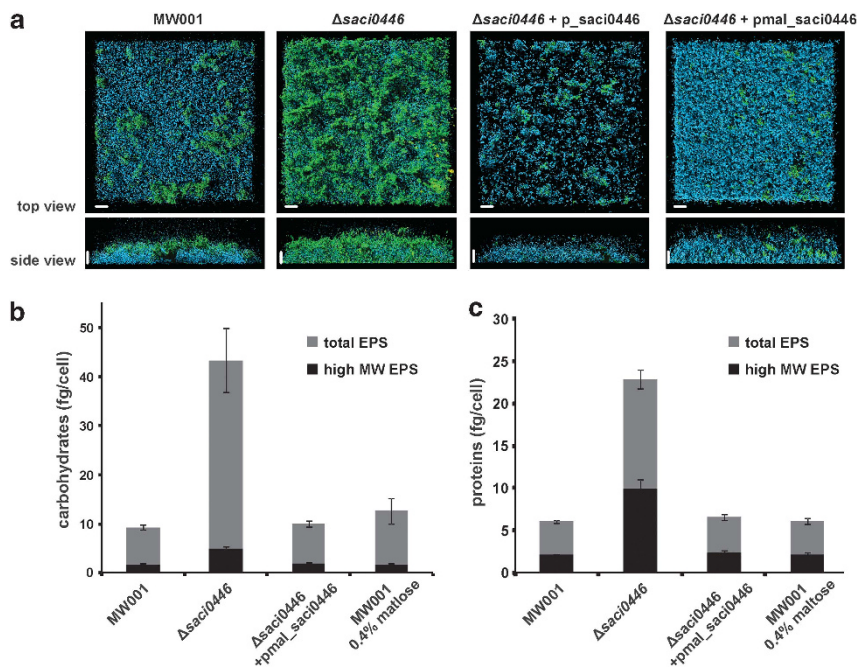


Figure 5 EPS analysis of the *S. acidocaldarius* deletion strain *saci0446*. (a) Three-day-old biofilms of trans-complemented Δ *saci0446* + *p_saci0446* and Δ *saci0446* + *pmal_saci0446* strains were analysed by CLSM and compared with the reference strain MW001 and Δ *saci0446* strains. Biofilm cells were stained using 4'-6-diamidino-2-phenylindole (blue), ConA (green) and IB4 (yellow). The overlay images of all three channels are shown. Scale bar = 20 μ m. (b) EPS were isolated from 3-day-old biofilms of MW001, Δ *saci0446*, Δ *saci0446* + *pmal_saci0446* and MW001 supplemented with 0.4% (w/v) of maltose. Carbohydrate concentrations were determined from both, non-dialyzed EPS (total EPS, gray bars) and dialyzed EPS extracts (3.5 kDa; high-molecular-weight EPS, black bars). (c) Protein concentrations of the same non-dialyzed and dialyzed EPS. The means and s.d. of three biological replicates are shown for b and c.

EPS characterization of biofilms formed by Δ *saci0446*

As already described, Δ *saci0446* deletion strain biofilms exhibited a prominent EPS production pattern (Figure 3), implying a regulatory role of *saci0446* in the control of EPS biosynthesis. To test this assumption, trans-complemented Δ *saci0446* deletion strains were subjected to CLSM analysis. The presence of *saci0446* under the control of its promoter (Δ *saci0446* + *p_saci0446*) indeed reduced the production of EPS (Figure 5a), and complementation with *saci0446* under overexpression conditions led to even lower EPS levels than apparent in the reference strain biofilms (Figure 5a). In addition, biofilms formed by the Δ *saci0446* + *pmal_saci0446* strain displayed higher cell densities when compared with the reference strain (Figure 5a).

To determine differences in composition and quantity of EPS components during biofilm formation, MW001, Δ *saci0446* and Δ *saci0446*-*pmal_saci0446* strains were grown as static biofilms and EPS were isolated using a cation exchange resin (Dowex). Subsequently, the carbohydrate and protein contents of the non-dialyzed cell-free EPS fractions (that is, total amount of extracellular carbohydrates and proteins including low-molecular-weight substances) and the dialyzed cell-free EPS fractions were determined (Figures 5b and c). The EPS of the reference strain MW001 contained a total carbohydrate concentration of 7.4 fg per cell. Most of the measured carbohydrates in MW001 were

of low molecular weight (≤ 3.5 kDa) and were thus removed by dialysis resulting in an EPS carbohydrate concentration of 1.8 fg per cell (Figure 5b). The mutant strain Δ *saci0446* displayed a fivefold higher carbohydrate production per cell (38.4 fg per cell), compared with the MW001 strain (Figure 5b). The carbohydrate levels of the EPS could be restored to wild-type levels in the trans-complemented Δ *saci0446* + *pmal_saci0446* recombinant strain (Figure 5b). To exclude an effect on EPS production by the presence of maltose that was needed for the expression of *saci0446*, the carbohydrate and protein content of the EPS content was also determined in MW001 cells grown in the presence of maltose. These controls did not show any changes when compared with MW001 grown in the absence of maltose (Figures 5b and c). In addition, protein quantification revealed a similar trend as observed for the carbohydrate content of the EPS in all tested strains (Figure 5c). The highest secretion of proteins was found in the Δ *saci0446* deletion strain, showing 12.9 fg per cell, with 76.8% being proteins of high molecular weight (Figure 5c). This analysis indicated that the extracellular biofilm matrix of the Δ *saci0446* deletion strain was highly enriched in both polysaccharides and proteins.

To date, no genes involved in EPS biosynthesis in archaea are known. However, the *S. acidocaldarius* genome contains a gene locus (*saci1904–1927*) encoding 11 glycosyltransferases and other genes

coding for enzymes involved in the modification and polymerization of sugars. Within this gene cluster, we focused on putative gene products, which share similarities with enzymes involved in bacterial exopolysaccharide biosynthesis and secretion (Figure 6a). Therefore, the differential expression profiles of those genes in Δ *saci0446* biofilm-associated cells in comparison with the reference strain MW001 were determined. Although transcript levels of *saci1908* were increased in the Δ *saci0446* deletion strain, transcription of *saci1909* was downregulated (Figure 6b). *saci1908* encodes a putative membrane protein exhibiting 15 transmembrane segments and *saci1909* encodes a putative glycosyltransferase sharing 28.8% sequence identity with a dolichyl-phosphate mannose synthase. The functions of these two gene products are still uncharacterized in *S. acidocaldarius*.

In order to shed light into the potential role of *saci1908* in *S. acidocaldarius* exopolysaccharide biosynthesis, double mutants using Δ *saci0446* as a background strain were generated for both *saci1908* (Δ *saci0446-saci1908*) and *saci1909* (Δ *saci0446-saci1909*). The distinctive Δ *saci0446* biofilm phenotype was reverted in Δ *saci0446-saci1908* and resembled reference strain MW001 biofilms (Figure 6c). In contrast to this, the deletion of *saci1909* led to an overproduction of unevenly distributed exopolysaccharides like in the Δ *saci0446-saci1909* deletion mutant. Therefore, both Saci1908 and Saci1909 might be involved in exopolysaccharide production in *S. acidocaldarius*, but that only Saci1908 is in the Saci0446 regulatory network as the phenotype of Saci1909 deletion is independent of Saci0446.

In vitro DNA-binding assays of Saci0446

To test whether Saci0446 is directly involved in the regulation of the genes that were differentially expressed in the Δ *saci0446* strain, Saci0446 was heterologously expressed and purified (Supplementary Figure 6). Electrophoretic mobility shift assays were performed with similar sized (about 185 bp) DNA probes containing either promoter regions of potential target genes *flaX* (*saci1177*), *flaB* (*saci1178*), *aapA* (*saci2314*), *saci1908* and the promoter region of the own gene (*saci0446*), or part of the *saci0446*-coding region as a specificity control (Figure 7a). Electrophoretic mobility shift assay with all probes resulted in the formation of multiple protein–DNA complexes with similar relative mobilities (Figure 7a). Binding affinities differed and were significantly higher for the promoter fragments (K_D in the range of 100–600 nM) than for the fragment containing the coding sequence (Table 2). Except for the latter fragment, a positive binding cooperativity was observed with Hill coefficients exceeding 1 (Table 2). In particular, Saci0446 bound to both its own promoter region and the promoter of *aapA* with comparable and the highest affinities ($K_D = 147$ nM and

134 nM, respectively). Footprinting assays are described in the Supplementary Material (Supplementary Figure 7).

In conclusion, Saci0446 binds DNA with a high affinity but low sequence specificity and the affinity of binding to potentially targeted promoter regions is higher than for a non-relevant DNA sequence. Therefore, it is probable that Saci0446 mediates regulation by cooperative binding at the promoter loci.

Discussion

From studies using bacterial models, it is now well recognized that microbial biofilm development involves coordinated events leading to well-defined and distinct phenotypes that must obey a tightly regulated genetic program. Although archaea are frequently detected in biofilm communities, the molecular bases that underlie the sessile lifestyle remain to be discovered. In this study, we described the identification and the initial characterization of six homologous transcriptional regulators named as Lrs14 regulators from *S. acidocaldarius* regarding their potential role during biofilm development. Our analyses unraveled that three of them (*saci1223*, *saci1242* and *saci0446*) are involved in regulating different aspects of biofilm development and that their mode of action presumably targets different pathways during this process in *S. acidocaldarius*. To our knowledge, this is the first report on regulatory components for the biofilm mode of growth in the archaeal domain.

In a previous study, we determined that the Lrs14 transcriptional regulator Saci1223 was one of the few common upregulated proteins among biofilm-grown *Sulfolobus* spp. (Koerdt *et al.*, 2011), thus suggesting its role as a key regulatory factor in biofilm development. Indeed, the deletion of this regulator resulted in *S. acidocaldarius* cells that were noticeably impaired to build biofilms (Figures 2 and 3). As CLSM analysis showed Δ *saci1223* was impaired in surface colonization (~50% less cells on the surface), suggesting that the assembly of surface structures may be perturbed (Henche *et al.*, 2011). However, none of the surface structure components, with the exception of *upsAE*, were found to be significantly altered in expression in biofilms formed by Δ *saci1223* (Figure 4a). Although *ups* pili are essential for ultraviolet-induced cell aggregation and DNA transfer (Fröls *et al.* 2008), their role in surface attachment from shaking cultures and during biofilm maturation was demonstrated (Henche *et al.*, 2011). However, Δ *ups* strains formed very unstable biofilms showing cell clusters unevenly distributed, which is different from Δ *saci1223* biofilms. Therefore, the deletion of *saci1223* might lead to a more complex pleiotropic response, which still has to be understood. In the future, additional analyses such as whole-transcriptional profiling of Δ *saci1223* biofilms at

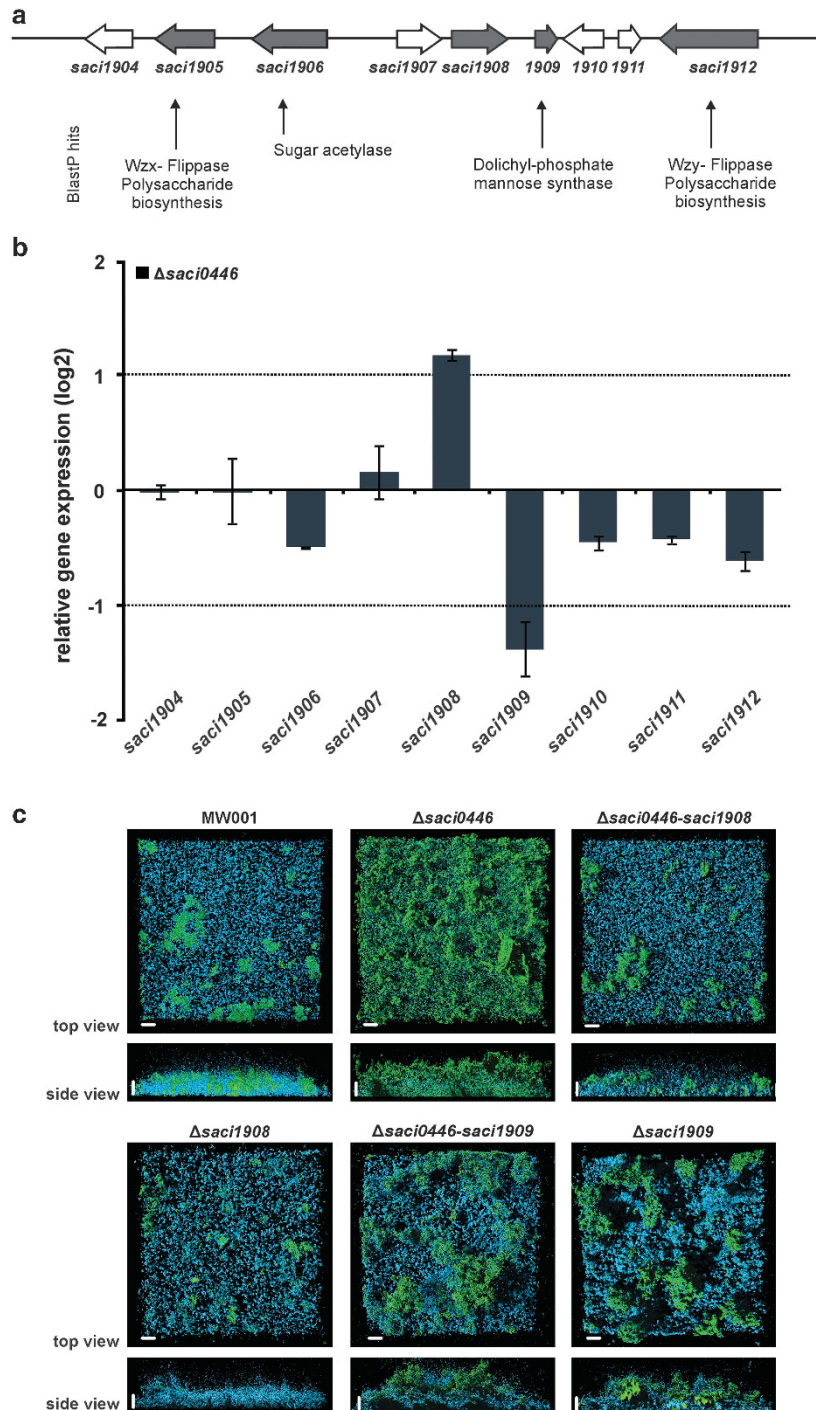


Figure 6 Analysis of *S. acidocaldarius* putative genes involved in EPS production. **(a)** EPS-related gene cluster of *S. acidocaldarius*. White arrows represent ORF with homology to glycosyl transferases encoding genes, whereas gray arrows correspond to ORFs which gene products share homology with proteins involved in bacterial EPS biosynthetic pathways. Best blast hits are indicated underneath. **(b)** Differential gene expression of EPS-related genes in the deletion strains Δ *saci0446* (black bars) during biofilm growth. The values reflect the fold change in expression compared with the reference strain MW001, which is designated as baseline. Relative transcript expression levels of each target gene were normalized to the internal control gene *secY*. **(c)** CLSM analysis of 3-day-old biofilm cultures of the double and single deletion mutants: Δ *saci0446-saci1908*, Δ *saci1908*, Δ *saci0446-saci1909* and Δ *saci1909*. Biofilm cells were stained using 4'-6-diamidino-2-phenylindole (blue), ConA (green) and IB4 (yellow). The overlay images of all three channels are shown. Scale bar = 20 μ m.

different maturation stages could shed light into the role of *Saci1223* during biofilm growth of *S. acidocaldarius*.

The deletion of *saci0446* led to one of the most intriguing and distinct phenotypes. Δ *saci0446* cells formed densely packed biofilms characterized by

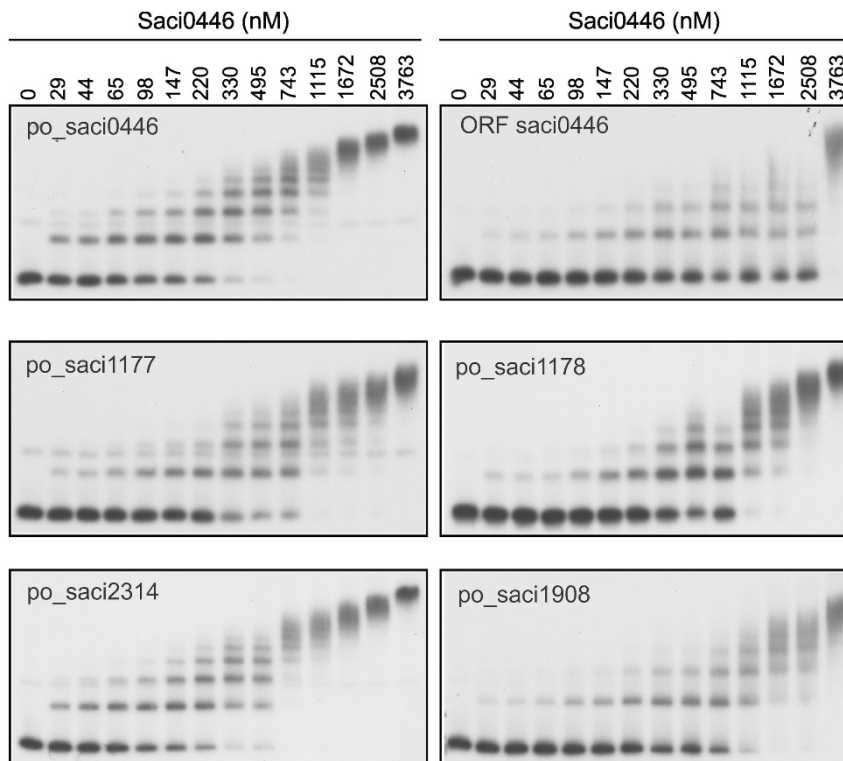


Figure 7 *In vitro* DNA-binding analysis of Saci0446. Electrophoretic mobility shift assays of DNA binding of saci0446 to various DNA fragments. Lengths of the tested probes are 173 bp (p/o *saci0446*), 186 bp (ORF *saci0446*), 187 bp (p/o *saci1177*), 193 bp (p/o *saci2314*), 185 bp (p/o *saci1178*) and 181 bp (p/o *saci1908*). Protein concentrations are identical for all assays (in monomeric nM concentrations). The position of the free DNA probe is indicated as F.

Table 2 Binding parameters of *saci0446*-DNA binding

DNA probe	K_D (nM)	n (Hill coefficient)
p/o <i>saci0446</i>	147	1.49
ORF <i>saci0446</i>	7.6×10^8	0.62
p/o <i>saci1177</i> (<i>flaB</i>)	319	2.15
p/o <i>saci1178</i> (<i>flaX</i>)	621	1.98
p/o <i>saci2314</i> (<i>aapA</i>)	134	2.09
p/o <i>saci1908</i>	634	1.88

secretion of larger amounts of EPS as well as their impaired motility (Figures 3, 4 and 6). As the lack of archaella does not affect biofilm formation in *S. acidocaldarius*, its primary role is in motility and not persistence on surfaces (Henne *et al.*, 2011). However, the upregulation of one pilin subunit (*aapA*), presumably resulting in increased numbers of the adhesive pili on the cell surface, could be the reason that the Δ *saci0446* deletion strain showed a much denser appearance in the CLSM analysis (Figure 3). This taken together with the augmented EPS amount leads to the very stout and packed Δ *saci0446* biofilms.

Saci0446 efficiently bound to the promoters of *flaB* and *aapA* genes and to its own promoter sequence, most likely acting as an activator for *flaB* and as repressor for *aapA*. In archaeellum regulation, the FHA domain-containing protein ArnA and the vWA domain-containing protein ArnB interact

strongly *in vivo* to consequently act as repressors of archaella expression (Reimann *et al.*, 2012). The data presented here indicates Saci0446 as another player in archaeellum regulation and implies that the archaeellum transcriptional regulation network seems to be more complex than previously envisaged.

The lack of Saci0446 led to an increased production of EPS (Figure 5). This could be either due to increased exopolysaccharide production (Figure 3) and/or a significant change in the glycosylation pattern of cell surface-associated or extracellular proteins. As mentioned before, an exopolysaccharide biosynthetic pathway has not yet been described for any archaeon. Here, we identified a gene locus (*saci1904–1927*) whose gene products shared similarities with enzymes involved in bacterial exopolysaccharide biosynthesis and secretion (Figure 6a). Via genetic epistasis analysis we could determine that the deletion of *saci1908* abolished EPS overproduction of the Δ *saci0446* deletion strain (Figure 6c), thus strongly suggesting that its gene product has a relevant role in the EPS biosynthetic pathways of *S. acidocaldarius*. As Saci0446 bound to the promoter region of *saci1908* and thereby would act as its repressor, as *saci1908* mRNA levels were increased in the Δ *saci0446* strain. Saci1908 is a putative membrane protein exhibiting 15 transmembrane regions with no function assigned so far. Therefore, it will be of great interest to unravel the

function of Saci1908 regarding its role during EPS production/secretion.

The dual role of Saci0446 in controlling cell motility and formation of biofilms is reminiscent of several bacterial models in which tight regulation exists between cell motility and biofilm formation. For instance in *Escherichia coli*, CsgD is a key transcriptional regulator for curli production as well as a master regulator of biofilm formation. CsgD was shown to directly repress gene expression of flagella components, and activate the synthesis of extracellular polysaccharides, thereby switching from planktonic growth to the biofilm mode (Zogaj *et al.*, 2001; Pesavento *et al.*, 2008). Moreover, CsgD modulates *adrA* upregulation, which encodes one of the enzymes for cyclic di-GMP synthesis (Ogasawara *et al.*, 2010). c-di-GMP consequently inhibits cell motility by interfering with the flagella motor speed via the c-di-GMP-binding protein YcgR (Wolfe and Visick, 2008; Boehm *et al.*, 2010). From our results, we can suggest that Saci0446 acts in a rather opposite manner when compared with CsgD from *E. coli*, as Saci0446 activates archaeal synthesis and represses genes required for biofilm formation.

In conclusion, this study reveals for the first time that members of the Lrs14 proteins, an archaea-specific class of transcriptional regulators, act in modulating the development of biofilms in *S. acidocaldarius*. In more detail, we demonstrated that *saci0446* most likely represses EPS production during biofilm growth, while activating cell motility; thereby we propose to name *saci0446* as *abfR1* (for Archaeal Biofilm Regulator 1) as our results clearly show its role in building and shaping biofilm communities of *S. acidocaldarius*.

Conflict of Interest

The authors declare no conflict of interest.

Acknowledgements

AO received a Max Planck Postdoctoral fellowship and SVA was supported by the Collaborative Research Center 987 by the DFG and by intramural funds of the Max Planck Society. EP is a postdoctoral fellow of the Research Foundation Flanders (Fonds Wetenschappelijk Onderzoek—Vlaanderen).

References

- Baker BJ, Banfield JF. (2003). Microbial communities in acid mine drainage. *Fems Microbiol Ecol* **44**: 139–152.
- Baker-Austin C, Potrykus J, Wexler M, Bond PL, Dopson M. (2010). Biofilm development in the extremely acidophilic archaeon *Ferroplasma acidarmanus* Fer1. *Extremophiles* **14**: 485–491.
- Bell SD, Jackson SP. (2001). Mechanism and regulation of transcription in archaea. *Curr Opin Microbiol* **4**: 208–213.
- Boehm A, Kaiser M, Li H, Spangler C, Kasper CA, Ackermann M *et al.* (2010). Second messenger-mediated adjustment of bacterial swimming velocity. *Cell* **141**: 107–116.
- Brock TD, Brock KM, Belly RT, Weiss RL. (1972). *Sulfolobus*: a new genus of sulfur-oxidizing bacteria living at low pH and high temperature. *Archiv fur Mikrobiologie* **84**: 54–68.
- Costerton JW, Lewandowski Z, Caldwell DE, Korber DR, Lappin-Scott HM. (1995). Microbial biofilms. *Annu Rev Microbiol* **49**: 711–745.
- Costerton JW, Stewart PS, Greenberg EP. (1999). Bacterial biofilms: a common cause of persistent infections. *Science* **284**: 1318–1322.
- Fröls S, Ajon M, Wagner M, Teichmann D, Zolghadr B, Folea M *et al.* (2008). UV-inducible cellular aggregation of the hyperthermophilic archaeon *Sulfolobus solfataricus* is mediated by pili formation. *Mol Microbiol* **70**: 938–952.
- Fröls S, Dyll-Smith M, Pfeifer F. (2012). Biofilm formation by haloarchaea. *Environ Microbiol* **14**: 3159–3174.
- Henche A-L, Koerdt A, Ghosh A, Albers SV. (2011). Influence of cell surface structures on crenarchaeal biofilm formation using a thermostable green fluorescent protein. *Environ Microbiol* **14**: 779–793.
- Justice NB, Pan C, Mueller R, Spaulding SE, Shah V, Sun CL *et al.* (2012). Heterotrophic archaea contribute to carbon cycling in low-pH, suboxic biofilm communities. *Appl Environ Microbiol* **78**: 8321–8330.
- Koerdt A, Gödeke J, Berger J, Thormann KM, Albers SV. (2010). Crenarchaeal biofilm formation under extreme conditions. *Plos One* **5**: e14104.
- Koerdt A, Jachlewski S, Ghosh A, Wingender J, Siebers B, Albers SV. (2012). Complementation of *Sulfolobus solfataricus* PBL2025 with an α -mannosidase: effects on surface attachment and biofilm formation. *Extremophiles* **16**: 115–125.
- Koerdt A, Orell A, Pham TK, Mukherjee J, Wlodkowski A, Karunakaran E *et al.* (2011). Macromolecular fingerprinting of *Sulfolobus* species in biofilm: a transcriptomic and proteomic approach combined with spectroscopic analysis. *J Proteome Res* **10**: 4105–4119.
- Kozubal MA, Macur RE, Jay ZJ, Beam JP, Malfatti SA, Tringe SG *et al.* (2012). Microbial iron cycling in acidic geothermal springs of yellowstone national park: integrating molecular surveys, geochemical processes, and isolation of novel Fe-active microorganisms. *Front Microbiol* **3**: 109.
- Lapaglia C, Hartzell PL. (1997). Stress-induced production of biofilm in the hyperthermophile *Archaeoglobus fulgidus*. *Appl Environ Microbiol* **63**: 3158–3163.
- Lassak K, Neiner T, Abhrajyoti G, Klingl A, Reinhard W, Albers SV. (2012). Molecular analysis of the crenarchaeal flagellum. *Mol Microbiol* **83**: 110–124.
- Lopez D, Vlamakis H, Kolter R. (2010). Biofilms. *Cold Spring Harb Perspect Biol* **2**: a000398.
- Napoli A, Van der Oost J, Sensen CW, Charlebois RL, Rossi M, Ciaramella M. (1999). An Lrp-like protein of the hyperthermophilic archaeon *Sulfolobus solfataricus* which binds to its own promoter. *J Bacteriol* **181**: 1474–1480.

- Ogasawara H, Yamamoto K, Ishihama A. (2010). Regulatory role of MlrA in transcription activation of *csgD*, the master regulator of biofilm formation in *Escherichia coli*. *FEMS Microbiol Lett* **312**: 160–168.
- Orcutt BN, Sylvan JB, Knab NJ, Edwards KJ. (2011). Microbial ecology of the dark ocean above, at, and below the seafloor. *Microbiol Mol Biol Rev* **75**: 361–422.
- Peeters E, Charlier D. (2010). The Lrp Family of Transcription Regulators in Archaea. *Archaea* **2010**: 750457.
- Pesavento C, Becker G, Sommerfeldt N, Possling A, Tschowri N, Mehli A *et al.* (2008). Inverse regulatory coordination of motility and curli-mediated adhesion in *Escherichia coli*. *Genes Dev* **22**: 2434–2446.
- Reimann J, Lassak K, Khadouma S, Ettema TJ, Yang N, Driessen AJ *et al.* (2012). Regulation of archaeella expression by the FHA and von Willebrand domain-containing proteins ArnA and ArnB in *Sulfolobus acidocaldarius*. *Mol Microbiol* **86**: 24–36.
- Schopf S, Wanner G, Rachel R, Wirth R. (2008). An archaeal bi-species biofilm formed by *Pyrococcus furiosus* and *Methanopyrus kandleri*. *Arch Microbiol* **190**: 371–377.
- Shock EL, Holland M, Amend JP, Meyer-Dombard DR. (2005). Geochemical sources of energy for microbial metabolism in hydrothermal ecosystems: Obsidian Pool, Yellowstone National Park, USA. *Geothermal Biol and Geochem Yellowstone Natl Park* (W. Inskeep, T. McDermott, eds.), Thermal Biology Institute, Montana State University. pp 95–112.
- Van Der Sluis EO, Nouwen N, Koch J, De Keyzer J, Van Der Does C, Tampé R *et al.* (2006). Identification of two interaction sites in SecY that are important for the functional interaction with SecA. *J Mol Biol* **361**: 839–849.
- Wagner M, Berkner S, Ajon M, Driessen AJ, Lipps G, Albers SV. (2009). Expanding and understanding the genetic toolbox of the hyperthermophilic genus *Sulfolobus*. *Biochem Soc Trans* **37**: 97–101.
- Wagner M, Van Wolferen M, Wagner A, Lassak K, Meyer BH, Reimann J *et al.* (2012). Versatile genetic tool box for the crenarchaeote *Sulfolobus acidocaldarius*. *Front Microbiol* **3**: 214. –.
- Wolfe AJ, Visick KL. (2008). Get the message out: cyclic-Di-GMP regulates multiple levels of flagellum-based motility. *J Bacteriol* **190**: 463–475.
- Zogaj X, Nimtz M, Rohde M, Bokranz W, Römling U. (2001). The multicellular morphotypes of *Salmonella typhimurium* and *Escherichia coli* produce cellulose as the second component of the extracellular matrix. *Mol Microbiol* **39**: 1452–1463.
- Zolghadr B, Weber S, Szabó Z, Driessen AJM, Albers SV. (2007). Identification of a system required for the functional surface localization of sugar binding proteins with class III signal peptides in *Sulfolobus solfataricus*. *Mol Microbiol* **64**: 795–806.

Supplementary Information accompanies this paper on The ISME Journal website (<http://www.nature.com/ismej>)